Extrapolation of extreme traffic load effects on bridges based on long-term SHM data

Y.X. Xia and Y.Q. Ni[*]

*Department of Civil and Environmental Engineering, The Hong Kong Polytechnic University,
Hung Hom, Kowloon, Hong Kong*

Abstract. In the design and condition assessment of bridges, it is usually necessary to take into consideration the extreme conditions which are not expected to occur within a short time period and thus require an extrapolation from observations of limited duration. Long-term structural health monitoring (SHM) provides a rich database to evaluate the extreme conditions. This paper focuses on the extrapolation of extreme traffic load effects on bridges using long-term monitoring data of structural strain. The suspension Tsing Ma Bridge (TMB), which carries both highway and railway traffic and is instrumented with a long-term SHM system, is taken as a testbed for the present study. Two popular extreme value extrapolation methods: the block maxima approach and the peaks-over-threshold approach, are employed to extrapolate the extreme stresses induced by highway traffic and railway traffic, respectively. Characteristic values of the extreme stresses with a return period of 120 years (the design life of the bridge) obtained by the two methods are compared. It is found that the extrapolated extreme stresses are robust to the extrapolation technique. It may owe to the richness and good quality of the long-term strain data acquired. These characteristic extremes are also compared with the design values and found to be much smaller than the design values, indicating conservative design values of traffic loading and a safe traffic-loading condition of the bridge. The results of this study can be used as a reference for the design and condition assessment of similar bridges carrying heavy traffic, analogous to the TMB.

Keywords: traffic load effects; extreme value; structural health monitoring; design validation; condition assessment

1. Introduction

A great deal of work has been done on evaluating the load-carrying capacity of bridges and the associated uncertainties. The load-carrying capacity generally depends on the construction quality, the strength of the structural components, and the operational loadings and environment. Long-term structural health monitoring (SHM) can offer an immense amount of site-specific information about these effects to quantify the uncertainty. Such information can be incorporated into time-dependent reliability-based condition assessment, facilitating the bridge maintenance and management. As one of the great sources of uncertainty, traffic load effects (TLEs) are the focus of this study. The TLEs mean strains/stresses or inner forces like bending moments, shear forces and

---

∗Corresponding author, Professor, E-mail: ceyqni@polyu.edu.hk

so on, resulting from highway and/or railway vehicles passing over a bridge. The effects due to loads of cars and other relatively light vehicles are unconcerned because they are usually not the dominant factor which threatens the serviceability and safety of bridges. On the contrary, the extreme effects arising under scenarios such as heavy vehicles crossing, several vehicles meeting or overtaking, and traffic jam are of the greatest interest.

In the context of probabilistic modeling, extreme values correspond to the tails of probabilistic distributions. The extreme value theory (EVT) develops techniques and models to describe these tails, and provides a framework to predict the characteristic values and probabilities of rare events on the basis of historical data. It has been widely applied in many fields such as hydrology, climate forecasting, finance and so on (Tawn 1990, Harris 1996, Tsimplis and Blackman 1997, Holmes and Moriarty 1999, Poon *et al.* 2004, Gilli 2006). The EVT has also been applied in bridge engineering to extrapolate extreme traffic loads or load effects (Bailey 1996, Crespo-Minguillón and Casas 1997, Bailey and Bez 1999, O'Connor 2001, Grave 2002, Getachew 2003, James 2003, Caprani 2005, Caprani *et al.* 2008, Enright 2010, Treacy *et al.* 2014). However, in most of the previous studies, the investigators addressed TLEs by generating the traffic loads based on weigh-in-motion (WIM) data collected during a short period and then predicting the load effects with the help of influence lines. The short-term data are unlikely to capture extreme events. On the other hand, the reliability of extreme values obtained by simulation techniques such as the Monte Carlo method is doubtful. Some uncertainties such as the dynamic impact of vehicles, the roughness of the road, and properties of structural materials are difficult to simulate in this procedure. Miao and Chan (2002) and Chan *et al.* (2005) have developed bridge live load models by using WIM data acquired over ten years. Their studies laid emphasis on the extrapolation of parameters about traffic loads, such as the gross weight and axle weight of the vehicles. Investigations on the extreme TLEs of long-span bridges based on long-term monitoring data were scarcely reported.

Strain monitoring data provides the most direct link to the load effect and avoids the difficulty in uncertainty modeling. In this study, the long-term strain data acquired by the SHM system deployed on the Tsing Ma Bridge (TMB) will be used to study the extreme TLEs on the bridge. The TMB with a main span of 1,377 m is currently the world's longest suspension bridge that carries both highway and railway traffic. It is the key linkage of the most important transport network in Hong Kong, which connects the international airport to the commercial centers. As a result, the traffic on this bridge is relatively busy and heavy. After completing the bridge construction in 1997, a sophisticated long-term SHM system was implemented on the TMB to monitor and evaluate the structural health of the bridge under in-service conditions (Wong 2004, Ko and Ni 2005, Ni *et al.* 2011). Up to now, this system has operated continuously and successfully for more than 18 years, and a rich database has been obtained.

With the long-term strain data collected from the stiffening deck system of the TMB, the extreme stresses caused by highway and railway traffic respectively are evaluated. Characteristic values of the extreme stresses with a return period of 120 years (the design life of the bridge) are derived by an EVT-based extrapolation. Both the block maxima (BM) approach and the peaks-over-threshold (POT) approach are employed to extrapolate the extreme stresses. These two methods are popular in the EVT context but have their respective pros and cons. In this study, the characteristic values of the extreme stress extrapolated using these two methods will be compared and discussed; and will further be compared with the stresses generated by design traffic loads, which are computed with the help of a 3D finite element model (FEM) of the bridge. The results of this study provide not only a site-specific estimation of the extreme TLEs for design validation and

condition assessment of the bridge, but also a reference for the design and condition assessment of bridges analogous to the TMB.

The remainder of the paper is organized as follows. Section 2 outlines the theoretical background of applying the EVT to study extreme TLEs. Section 3 briefs the TMB and the deployed sensors for strain monitoring. In section 4, the strain monitoring data continuously collected in nine years are presented to observe long-term variations of the structural strains/stresses caused by highway and railway traffic, respectively. In section 5, characteristic values of the extreme stresses with a 120-year return period are extrapolated using the BM and POT approaches, respectively. The results of the two methods are compared and discussed. Furthermore, the characteristic extremes are compared with the design values with the aid of an FEM. Finally, conclusions are given in section 6.

2. Theory and methodology

A number of methods have been proposed to extrapolate the characteristic values of extremes. Among them, two methods, namely, the block maxima (BM) approach and the peaks-over-threshold (POT) approach, are most popular (Simiu *et al.* 2001, Katz *et al.* 2002, Getachew 2003, James 2003, Gindy and Nassif 2006, Messervey *et al.* 2011). In the BM approach, only the maximum values in given blocks of time (days, months, years, etc.) are taken into account. The BM approach has the advantage of time referencing, which is necessary in calculating probabilities of exceedance during the lifetime of a structure. Nonetheless, only one value in each time-block is considered even if several very large values were recorded; so a lot of useful data might be wasted. The POT approach accounting for the peaks which exceed a specified threshold can address the above issue, but its time reference is not as clear as the BM approach. The BM and POT data are often fitted to the generalized extreme value (GEV) distribution and the generalized Pareto (GP) distribution, respectively (Coles 2001, Beirlant *et al.* 2006). References on the EVT and its engineering applications are available (Gumbel 1958, Castillo 1988, Coles 2001, Reiss *et al.* 2001, Leadbetter *et al.* 2012).

2.1 GEV fitting and GP fitting

When the TLEs can be treated as a sequence of independent random variables $(X_1, X_2, \ldots, X_n)$ with a common distribution function F, one way for extrapolating the characteristic value of the extreme TLE is to explore the statistical behavior of

$$M_n = \max\left(X_1, X_2, \ldots, X_n\right) \tag{1}$$

where M_n represents the maximum of the observed data over n observations. In theory, the distribution of M_n can be expressed as

$$P(M_n \le z) = P(X_1 \le z, \ldots, X_n \le z) = P(X_1 \le z) \times \ldots \times P(X_n \le z) = F^n(z) \tag{2}$$

However, $F(z)$ is usually unknown in practice. To calculate $F^n(z)$, an approach is to accept that $F(z)$ is unknown, and to estimate only $F^n(z)$ based on the extreme data. This idea is similar to the central limit theorem.

To overcome the difficulty that $F^n(z)$ degenerates to 0 as n tends to infinity, the following linear renormalization of the variable M_n is introduced

$$M_n^* = \frac{M_n - b_n}{a_n} \tag{3}$$

where $\{a_n\}$ and $\{b_n\}$ are sequences of constants with $a_n > 0$. The limit distribution for M_n^* is given by the extreme types theorem (Jenkinson 1955) as follows: if there exist sequences of constants $\{a_n\}$ and $\{b_n\}$ such that

$$P\{(M_n - b_n)/a_n \leq z\} \xrightarrow{n \to \infty} G(z) \tag{4}$$

where G is a non-degenerate distribution function, then G is a distribution of the GEV family

$$G(z) = \exp\left\{-\left(1 + \xi\left(\frac{z - \mu}{\sigma}\right)\right)^{-1/\xi}\right\} \tag{5}$$

defined on z such that $1 + \xi(z-\mu)/\sigma > 0$, where $-\infty < \mu < \infty$, $\sigma > 0$ and $-\infty < \xi < \infty$. The three parameters μ, σ, and ξ are location, scale and shape parameters, respectively. Eq. (5) is called the GEV distribution. The cases $\xi = 0$, $\xi > 0$, and $\xi < 0$ are named the extreme value distribution (EVD) with types *I*, *II* and *III*, which are also widely known as Gumbel, Fréchet and Weibull families, respectively. The three types of EVDs have different forms of tail behavior. The upper bound is finite for the Weibull distribution while it is infinite for the Fréchet and Gumbel distributions.

Another way to extrapolate the characteristic value of the extreme TLE based on observations is to study the statistical behavior of those data that surpass a threshold level u. This statistical behavior can be described by the conditional probability

$$F_u(y) = P(X \leq u + y | X > u) = \frac{F(u + y) - F(u)}{1 - F(u)} \tag{6}$$

The following theorem (Balkema and De Haan 1974, Pickands III 1975) gives an approximation to the above probability when u is large enough: let $X_1, X_2, \ldots, X_n$ be a sequence of independent and identically distributed random variables and $M_n = \max\{X_1, X_2, \ldots, X_n\}$ satisfying the conditions to be approximated by a GEV distribution, then for a large u the distribution function of $(X - u)$ conditional on $X > u$, is approximately

$$H(y) = 1 - \left(1 + \xi y / \hat{\sigma}\right)^{-1/\xi} \tag{7}$$

defined on $\left\{y / y > 0 \text{ and } (1 + \xi y / \hat{\sigma}) > 0\right\}$ where

$$\hat{\sigma} = \sigma + \xi(u - \mu) \tag{8}$$

The family of distribution defined by Eq. (7) is called the GP distribution. The parameters of the GP distribution are uniquely determined by those of the associated GEV distribution. In

particular, the shape parameter ξ in Eq. (7) is equal to that of the corresponding GEV distribution. The shape parameter ξ determines the upper bound of the GP distribution in the same way as that of the GEV distribution.

2.2 Return level and return period

The quantile function z_p of the GEV distribution can be obtained by inverting Eq. (5) as

$$
z_p = \begin{cases} \mu - (\sigma / \xi)(1 - (-\log(1-p))^{-\xi}) & \text{for} \quad \xi \neq 0 \\ \mu - \sigma \log(-\log(1-p)) & \text{for} \quad \xi = 0 \end{cases}
\tag{9}
$$

where $G(z_p)=1-p$. In common terminology, z_p is the return level associated with the return period l/p. The return period is of significance in engineering due to the fact that it is usually used as a design criterion. By defining $y_p=-\log(1-p)$, Eq. (9) can be expressed as

$$
z_p = \begin{cases} \mu - (\sigma / \xi)(1 - y_p^{-\xi}) & \text{for} \quad \xi \neq 0 \\ \mu - \sigma \log y_p & \text{for} \quad \xi = 0 \end{cases}
\tag{10}
$$

If z_p is plotted against $\log y_p$, the plot is linear in the case of $\xi=0$; convex in the case of $\xi<0$ with an asymptotic limit as $p \to 0$ at $\mu-\sigma/\xi$; and concave in the case of $\xi>0$ without finite bound. This graph is named as return level plot, which is particularly convenient and useful for model presentation and validation.

For the case of the GP distribution, when $\xi \neq 0$ the return level x_m that is exceeded once on average for every m observations is

$$
x_m = u + \frac{\sigma}{\xi}\left(\left(m\varsigma_u\right)^\xi - 1\right)
\tag{11}
$$

and when $\xi=0$ the return level x_m is

$$
x_m = u + \sigma \log\left(m\varsigma_u\right)
\tag{12}
$$

where $\varsigma_u = P\{X>u\}$. As return level plots for the GEV model, plotting x_m against m on a logarithmic scale produces the same qualitative features: linearity if $\xi=0$; concavity if $\xi>0$; and convexity if $\xi<0$. To get the N-year return level, it is often more convenient to give return levels on an annual scale. For the m observations corresponding to n_y observations per year

$$
m = N \times n_y
\tag{13}
$$

Therefore the N-year return level is

$$
z_N = u + \frac{\sigma}{\xi}\left(\left(Nn_y\varsigma_u\right)^\xi - 1\right)
\tag{14}
$$

for $\xi \neq 0$; and is

$$z_N = u + \sigma \log\left(Nn_y \varsigma_u\right) \tag{15}$$

for $\xi = 0$.

2.3 Parameter estimation

The maximum likelihood estimation (MLE) is often adopted to estimate the parameters of the fitted model of extreme values. For the GEV model, the log-likelihood of the distribution when $\xi \neq 0$ is

$$L(\mu,\sigma,\xi) = -m\log\sigma - (1+1/\xi)\sum_{i=1}^{m}\log\left(1+\xi\frac{z_i-\mu}{\sigma}\right) - \sum_{i=1}^{m}\left(1+\xi\frac{z_i-\mu}{\sigma}\right)^{-1/\xi} \tag{16}$$

provided that

$$\left(1+\xi\frac{z_i-\mu}{\sigma}\right) > 0 \tag{17}$$

When Eq. (17) is violated, the likelihood is zero and the log-likelihood is minus infinity. For the Gumbel case ($\xi=0$), the log-likelihood is

$$L(\mu,\sigma) = -m\log\sigma - \sum_{i=1}^{m}\left(\frac{z_i-\mu}{\sigma}\right) - \sum_{i=1}^{m}\exp\left(-\frac{z_i-\mu}{\sigma}\right) \tag{18}$$

For the GP distribution, denoting the k excesses over the threshold u by $y_1, y_2, \ldots, y_k$, the log-likelihood function in the case of $\xi \neq 0$ is

$$L(\sigma,\xi) = -k\log\sigma - (1+1/\xi)\sum_{i=1}^{k}\log(1+\xi y_i/\sigma) \tag{19}$$

when $(1+\xi y_i/\sigma) > 0$; otherwise, $L(\sigma,\xi) = -\infty$. For $\xi=0$,

$$L(\sigma,\xi) = -k\log\sigma - \sigma^{-1}\sum_{i=1}^{k}y_i \tag{20}$$

By maximizing the log-likelihood functions defined in Eqs. (16) and (18)-(20), the MLE of the model parameters is obtained. Confidence intervals and other forms of inference can be obtained from the approximate normal distribution of the estimators. Return level inference can also be set using the normal approximation of the estimators. However, the normal approximation may be poor, especially for the return levels of long return periods. In this situation, a better approximation can be obtained by the profile likelihood function (Coles 2001, Leadbetter *et al.* 2012).

2.4 Model checking

There are four data-based plots to assist model checking: probability plot, quantile plot, return level plot and density plot. A probability plot is a comparison of the empirical and fitted probabilities of the extreme values. A successful probability plot should lie close to the unit diagonal. A weakness of the probability plot is that it provides the least information in the most concerned region, which corresponds to extremes with long return periods. This deficiency is avoided by the quantile plot. A quantile plot is a comparison of the empirical and fitted quantiles of the extreme values. Departure from linearity in the quantile plot also indicates model failure. The return level plot has been introduced in section 2.2. Empirical estimates of the return level are added to the plot. If the fitted model is suitable for the data, the model-based curve and empirical estimates should be in reasonable agreement. Confidence intervals can be added to the plot to increase its informativeness. For completeness, another diagnostic plot, the density plot which is based on the density function, is also adopted. By comparing the probability density function (PDF) of the fitted model with the histogram of the data, the fitted model can be validated. It is generally less informative than the previous plots, because the histogram can vary substantially with the choice of size of blocks or threshold of peaks.

2.5 Threshold selection for POT model

Like the choice of block size in the BM approach, threshold selection in the POT approach is also subjective. The selection implies a trade-off between bias and variance. When the threshold level is too low, the fitted model of extreme values is quite poor, leading to bias in estimation and extrapolation. On the other hand, overly high threshold levels generate only few data to derive the model, leading to large estimation variance. Two methods are popular to select the threshold: one is an exploratory technique carried out prior to model estimation; the other is an assessment of the stability of parameter estimates based on the fitting of models across a range of different thresholds (Coles 2001, Leadbetter *et al.* 2012, O'Brien *et al.* 2015). The first method builds the mean residual life plot representing the points (Coles 2001)

$$\left(u, \sum_{i=1}^{n_u} \left(x_{(i)} - u \right) \Big/ n_u \right) \qquad u < x_{\max} \tag{21}$$

where $x_{(i)}$ is the n_u observations that exceed u, and $x_{\max}$ is the maximum observation in the data set. Then the value of u above which the plot is approximately linear is chosen as the threshold. The representation of confidence intervals can help to determine this point. Sometimes mean residual life plots are difficult to be used as a method of threshold selection. A complementary technique is to fit the GP distribution over a range of thresholds, and then to look for stability of parameter estimates. The lowest value of u for which the parameter estimates of the GP model remain near-constant is selected as the threshold.

3. Tsing Ma Bridge and monitoring of strain

3.1 Tsing Ma Bridge

As shown in Fig. 1, the TMB is a suspension bridge with an overall length of 2,160 m and a main span of 1,377 m between the Tsing Yi tower in the east and the Ma Wan tower in the west. It is currently the world's longest suspension bridge that carries both highway and railway traffic. The bridge deck is a streamlined box-shaped and continuous truss girder with a central air-gap. It has a continuous length of 2,160 m and a total steel weight of 49,000 tonnes. The truss girder has two types of trusses, i.e., the Warren truss in the longitudinal direction and the Vierendeel truss in the transverse direction (Figs. 1(b) and 1(c)). The two longitudinal trusses link up the cross frames with 4.5 m apart from each other along the bridge longitudinal axis, acting as the main girder of the bridge. As shown in Fig. 1(b), the deck has two levels: the upper level carries a dual three-lane highway, and the lower level carries two railway tracks and two single-lane carriageways. At the main span and the Ma Wan side span, the deck is suspended from the main cables at 18 m intervals, i.e., at every four cross frames. The supports for the deck at the end of Ma Wan span, Ma Wan tower, Tsing Yi tower and piers, and the end of Tsing Yi span are: hinged support, rocker bearing, sliding bearing, and roller support in accordance with a highway movement joint at upper deck and a railway movement joint at lower deck, respectively. The movement joints at the end of Tsing Yi span is designed to accommodate the longitudinal displacement of the deck due to temperature variation.

The TMB serves a port and airport complex, so it carries a particularly large amount of heavy lorries. In normal days, the highway traffic is on the upper deck; while when there is a strong typhoon, the traffic on the upper deck will be closed and the two carriageways on the lower deck will be used for emergency. The vehicles running on the bridge are classified into eight categories according to their main features, including the number of axles, magnetic vehicle length, axle distance, and gross vehicle weight (GVW). The highway traffic on the TMB is governed by the Hong Kong road traffic regulations (HKRTR), so the maximum GVW and axle load of the vehicles are regulated. Before 2003, most trains passing through the TMB were 7-car trains; however, with the increasing demand of passenger flow, most trains had become 8-car trains since the end of 2005. The years between 2003 and 2005 were a transition period with 7-car and 8-car trains running concurrently. The railway traffic is managed by the MTR Corporation Limited, Hong Kong. The maximum distribution of bogie loads in an 8-car MTRC train is regulated, and the maximum gross train weight (GTW) allowed to pass the TMB is 498 tonnes.

3.2 Strain monitoring

A long-term SHM system called Wind And Structural Health Monitoring System (WASHMS) was installed on the TMB after the completion of its construction. Since its implementation in 1997, the SHM system has operated continuously and successfully for more than 15 years up to now. As an important part of this system, a total of 110 strain gauges have been installed in three selected deck sections, i.e., sections A, B and C as shown in Fig. 1(a), to measure the strain responses of the stiffening deck system under in-service loads. The strains of critical structural elements, such as chord members of the longitudinal trusses and cross frames, plan bracing members, deck trough and rocker bearings at the Ma Wan tower, in these three sections are measured. The strain gauges installed are in three types of configuration: single strain sensor (SS), pair strain sensor (SP), and rosette strain sensor (SR). Fig. 2 illustrates the deployment of strain gauges on the north and south longitudinal trusses at section C. The strain gauges are of electrical-resistance type with a model of LWK-06-W250B-350. They collect strain data at a

sampling rate of 51.2 Hz.

In mechanics, strain is a geometrical measure of deformation representing the relative displacement between particles in a material body (Lubliner 2008). It is a reflection of the loadings imposed on a structure, and can be used to directly calculate the inner forces of the structural components. For example, under the assumption of vertical bending at elastic state, the inner forces of the top and bottom chords as shown in Fig. 2 can be calculated by

$$P = EA\varepsilon_a = EA(\varepsilon_T Z_T + \varepsilon_B Z_B)/(Z_T + Z_B) \tag{22}$$

and

$$M = EZ_B\varepsilon_{bB} = (\varepsilon_T - \varepsilon_B)/(1/Z_T + 1/Z_B) \tag{23}$$

(a) Elevation view

(b) Warren truss

(c) Vierendeel truss

Fig. 1 General structural features of TMB
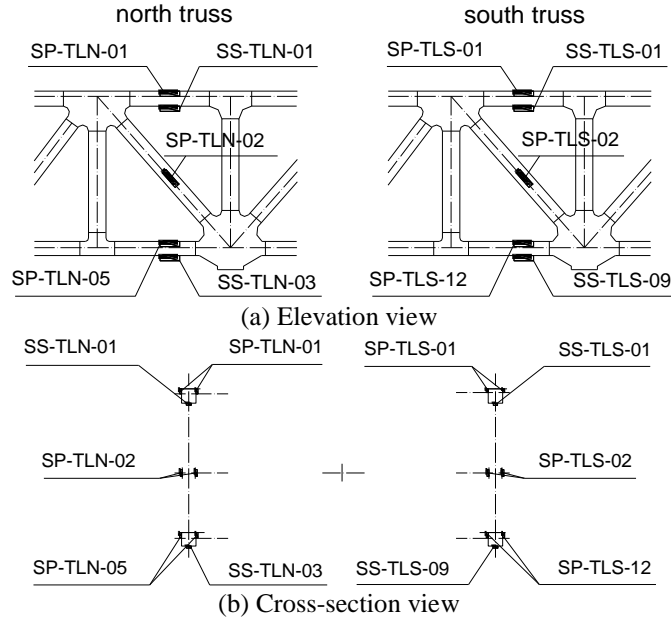
(a) Elevation view

(b) Cross-section view

Fig. 2 Strain gauges installed on longitudinal trusses on main span

where P is the axial force; M is the vertical bending moment; A is the area of the cross section; E is the elastic modulus of steel; ε_a is the average strain in the cross section; ε_T and ε_B are the strains measured by strain gauges at the upper and lower sides of a chord, respectively; Z_T and Z_B are the section moduli with respect to the positions of the strain gauges; and ε_{bB} is the bending strain at the bottom of the cross section. The axial force in the diagonal chords can be calculated by

$$P = EA\varepsilon_a = EA\left[(\varepsilon_1 + \varepsilon_2)/2\right] \tag{24}$$

where ε_1 and ε_2 are strains measured by strain gauges at the two opposite sides of a chord. The inner forces of the whole cross-section of the deck can be derived subsequently based on force equilibrium. The obtained inner forces (i.e., live load demand) can be incorporated for bridge condition assessment based on either provisions or structural reliability theory. The load and resistance factor rating factor (LRFR) is widely used in bridge provisions (AASHTO 2001, 2015, CSA 2006). According to these specifications, the LRFR for an existing bridge is

$$LRFR = \frac{\phi R_n - \gamma_D D_n}{\gamma_L L_n} \tag{25}$$

where R_n is nominal resistance; D_n and L_n are the nominal values of dead and live load effects, respectively; γ_D and γ_L are load factors for rating. The live load effect in Eq. (25) can be derived from the measured strains with the help of Eqs. (22) to (24). In structural reliability analysis, the performance function (limit state function or safety margin) is often written as

$$M(t) = R(t) - S(t) \tag{26}$$

where $M(t)$ is the safety margin; $R(t)$ and $S(t)$ represent the time-dependent resistance and load effects, respectively. The reliability is the probability, $P(M(t) \geq 0)$; thus the probabilistic distribution of the strain-derived live load effects is valuable to evaluate the structural reliability.

4. Variation tendency of long-term stresses

The strain acquired from the TMB deck is mainly due to four effects: highway traffic, railway traffic, wind, and temperature (Ni *et al.* 2011, Xia *et al.* 2012). The static strain resulting from initial dead loads is not measurable because the strain gauges were installed after the completion of bridge construction. The temperature-induced strain, although fairly large, contributes little to the stress because the majority of it is released by free movement of the bridge deck at the expansion joints on the Tsing Yi abutment. Therefore, under normal conditions, i.e. when there are no special events such as typhoons, the measured stress of the bridge deck is mainly due to highway and railway traffic. In recognition of the fact that the bridge performs in elastic stage under normal in-service conditions, the stress experienced by the steel trusses can be obtained from the measured strain by the Hooke's law. Characteristics of the strain measured at the three deck sections can be found in Ni and Xia (2016). It was found through statistical analysis of one-year strain data that the traffic-induced stresses in the longitudinal trusses at sections A and C are close to each other, while those at section B are smaller. For sections A and C, the bottom chords experienced larger stress than the top and diagonal chords. In addition, for the north and south bottom chords that are symmetric to each other against the longitudinal axis of the deck, the daily maximum stresses are close to each other. In this study, the strain measured by the strain gauge SSTLS09 (Fig. 2), which is a single strain gauge installed at the bottom of the longitudinal truss at section C, is selected to investigate the extreme TLEs on the TMB.

The measured strain data are inevitably contaminated with noise, spike and trend. Furthermore, to enable the study on the effects of highway and railway traffic individually, the strain should be decomposed first. In the present study, a wavelet-based signal pre-processing method in terms of denoising, despiking and decomposing is applied to obtain the desired signal, while the data errors observed are corrected using a method combining FEM analysis and multi-sensing signals. Fig. 3 shows the scatter plots of the daily maximum tensile stresses induced by highway and railway traffic, respectively. The data shown were measured during the period from April 2004 to December 2012, and have excluded those collected during typhoons and strong monsoons. It is found that the stresses due to highway traffic do not change much during the observed period. On the other hand, the railway-induced stresses have an increase during April 2004 to December 2006, but afterward there is no significant change. It is because 2005 is the critical year of pattern transition of the railway traffic on the TMB. Between 2003 and 2005, both 7-car and 8-car trains ran concurrently on the TMB, while after 2005 most of the trains running on the TMB were 8-car trains.

5. Extrapolation of extreme traffic load effects

The data acquired from April 2004 to December 2012 are used to extrapolate the extreme TLEs. A previous study has indicated that there is an increase in the strain during the years from 1999 to

2005. Fig. 4 shows the variation of monthly maximum and minimum inner forces which are calculated using the data collected during 1999 and 2005 by the strain gauges installed on an outer rocker bearing at the Ma Wan tower. The positive values indicate compressive forces, while the negative ones denote tensile forces. The monthly maximum compressive forces are mainly caused by the railway traffic. An increase of the compressive forces, and therefore the railway traffic loading from 1999 to 2005 is observed in Fig. 4. However, this increase did not continue after 2006 as shown in Fig. 3(b). It can be reasonably presumed that the railway loading on the TMB will not increase remarkably in the future, because the recorded maximum GTW during the period of 2004 to 2012 has exceeded 500 tonnes, which is heavier than the allowable maximum GTW (498 tonnes) prescribed by the MTR Corporation.

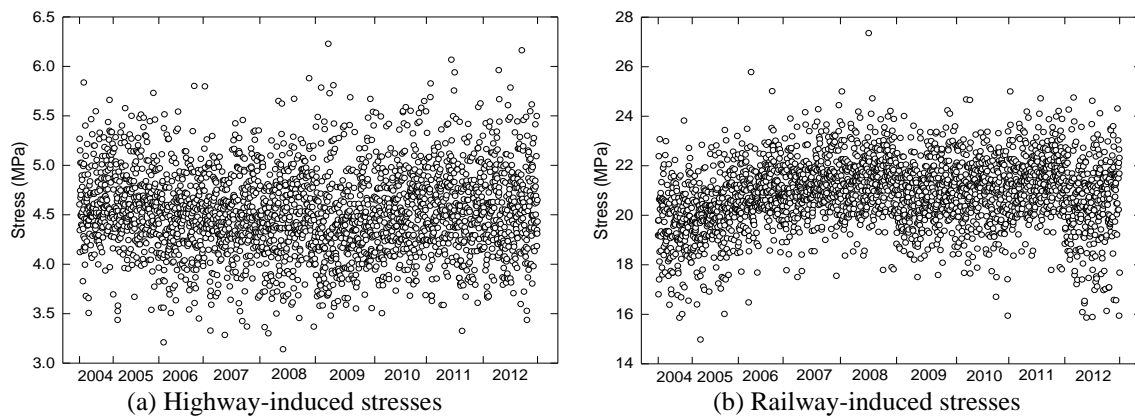(a) Highway-induced stresses   (b) Railway-induced stresses

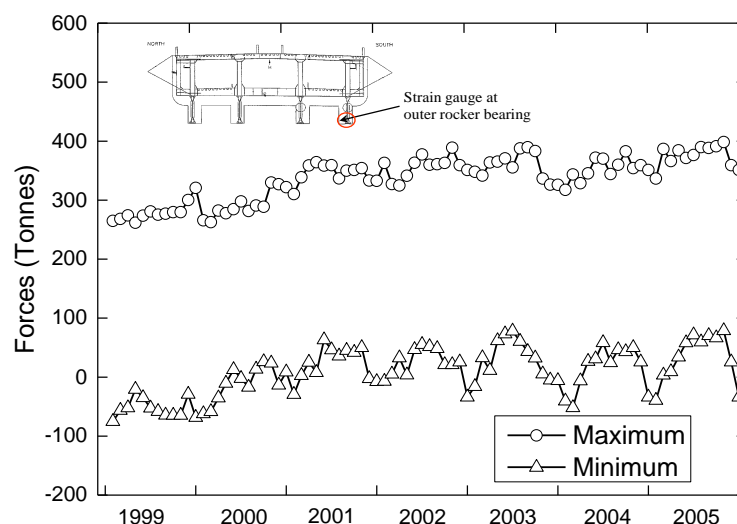Fig. 3 Scatter plots of daily maximum tensile stresses induced by highway and railway traffic

Fig. 4 Variation of monthly maximum and minimum inner forces during 1999 to 2005 calculated from measured strain data

The highway-induced stresses before 2004 are assumed not larger than those measured after 2004. A close circuit television video (CCTV) system has been installed to monitor the traffic on the bridge. According to the record of the CCTV, the highway traffic has been very dense sometimes in the daytime. As the TMB serves a port and airport complex, the bridge has carried a particularly large amount of heavy lorries. According to the weigh-in-motion (WIM) data, the percentage of the goods vehicles passing the bridge has exceeded 30% in some durations. Moreover, vehicles with their GVW heavier than the allowable maximum GVW stipulated in the HKRTR were recorded from time to time. In this regard, it is assumed that the highway loading on the TMB will not grow significantly in the future. The highway- and railway-induced stresses measured during 2004 and 2012 are used in the present study to predict the extreme values. The extreme value analysis is conducted by means of the package extRemes (Gilleland and Katz 2011) encoded with the open-source software environment R (R Development Core Team 2014).

5.1 Extrapolation using BM approach

The block-size to specify the extreme stresses using the BM approach is selected as one month. The scatter plot of the monthly maximum tensile stresses derived using the strain monitoring data from the strain gauge SSTLS09 is shown in Fig. 5, in which Fig. 5(a) is the highway-induced stresses, and Fig. 5(b) is the railway-induced stresses. From Fig. 3, it is observed that the daily maximum tensile stresses due to either highway or railway traffic can be considered to be statistically independent and identically distributed. As a result, the asymptotic distributions of the monthly maximum tensile stresses can be assumed to comply with the GEV distribution. The parameters of the distribution are estimated by the maximum likelihood method with the results given in Table 1. The diagnostic plots (probability plot, quantile plot, return level plot, and density plot) for the GEV fitting to the extreme stresses are shown in Fig. 6. In the return level plot, the 95% confidence intervals are also provided (grey dashed lines). It can be seen in Fig. 6 that the monthly maxima of both the highway-induced and railway-induced stresses are well fitted to the GEV distribution. By applying the profile likelihood method, the return level of the highway-induced stresses corresponding to a return period of 120 years (design life of the bridge) is determined to be 6.43 MPa, and that of the railway-induced stresses is 27.21 MPa. The 95% confidence intervals for these two return levels are [6.21, 7.07] and [26.58, 29.23], respectively.

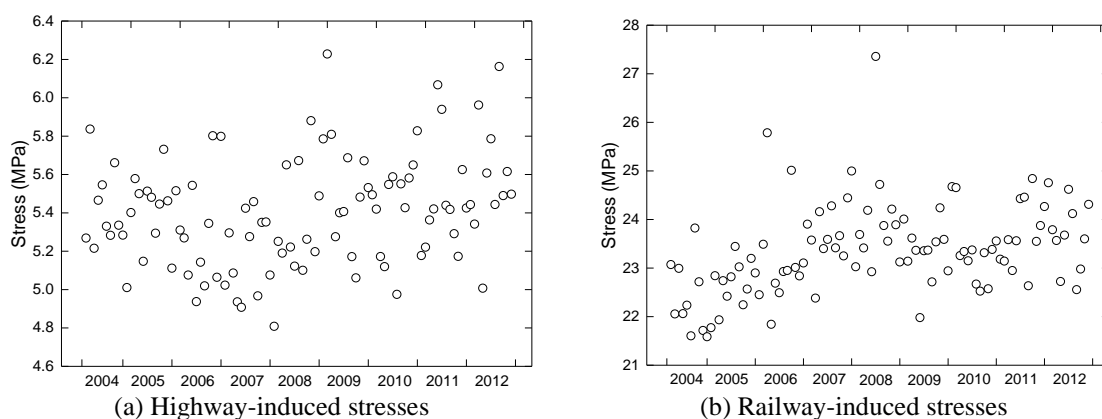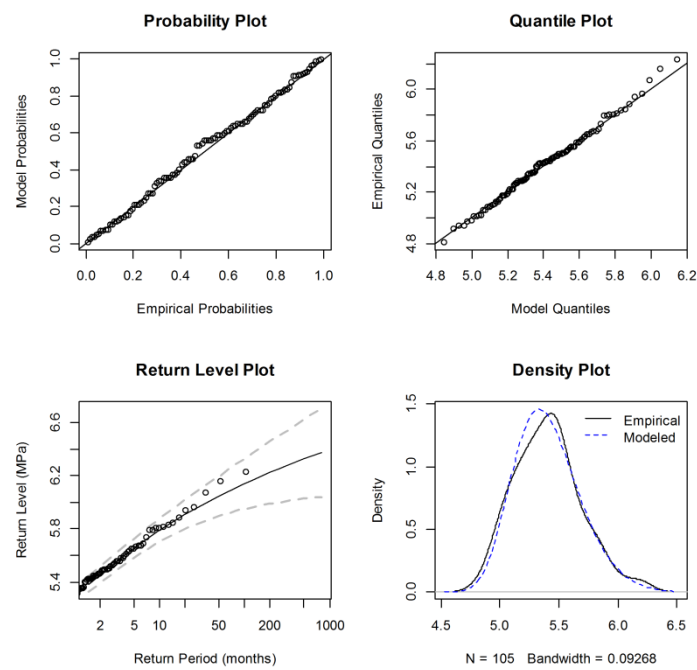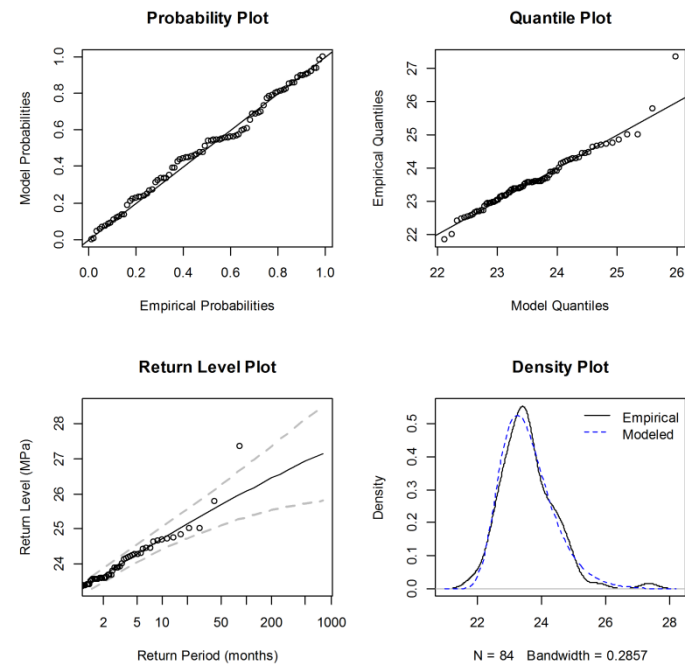(a) Highway-induced stresses   (b) Railway-induced stresses

Fig. 5 Scatter plots of monthly maximum tensile stresses due to highway traffic and railway traffic

(a) Highway-induced stresses

(b) Railway-induced stresses

Fig. 6 Diagnostic plots for GEV fitting to extremes of traffic-induced stresses

Table 1 Parameter estimate of GEV distribution for traffic-induced stresses

	μ	σ	ξ
Highway-induced	5.29	0.26	-0.15
Railway-induced	22.98	0.79	-0.09

5.2 Extrapolation using POT approach

The two threshold-selection techniques introduced in section 2.5 are employed to determine the thresholds for extreme extrapolation using the POT approach. The plots used to select the threshold of the daily maximum railway-induced stresses are shown in Fig. 7, in which Fig. 7(a) is the mean residual life plot, and Fig. 7(b) is the threshold range plot. According to the selection criteria described in section 2.5, the threshold is determined as 22.0 MPa. Similarly, the threshold for the model of the daily maximum highway-induced stresses is determined as 5.3 MPa. Again, the parameters of the GP distribution when using the POT approach for extreme extrapolation are estimated by the maximum likelihood method. The parameter estimation results are given in Table 2. The diagnostic plots for the GP fitting to the extreme stresses are provided in Fig. 8. It can be seen that the POTs of both the highway-induced and railway-induced stresses are well fitted to the GP distribution. Making use of the profile likelihood method, the return level of the highway-induced stresses with a 120-year return period is estimated to be 6.36 MPa; and that of the railway-induced stresses is 27.25 MPa. The 95% confidence intervals for these two return levels are [6.21, 7.10] and [26.58, 29.40], respectively.

Table 2 Parameter estimation of GP distribution for traffic-induced stresses

	σ	ξ
Highway-induced	0.24	-0.15
Railway-induced	0.79	-0.09

(a) Mean residual life plot   (b) Threshold range plot
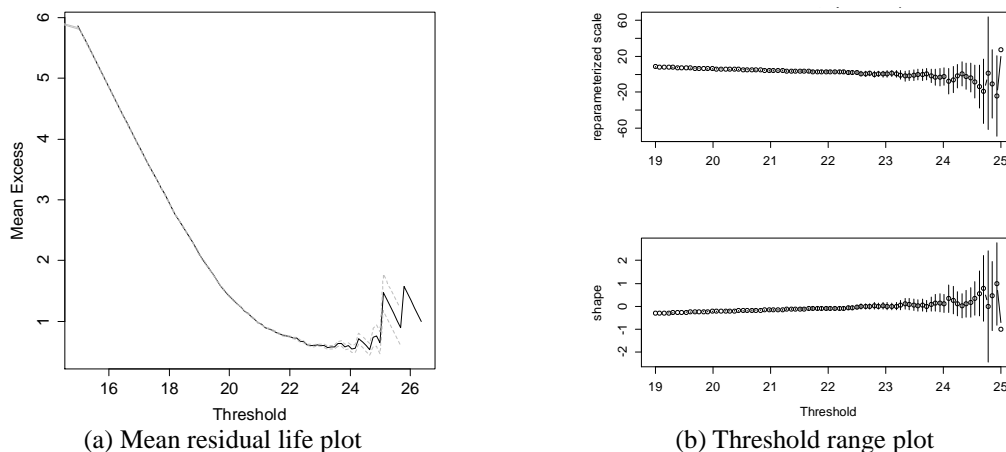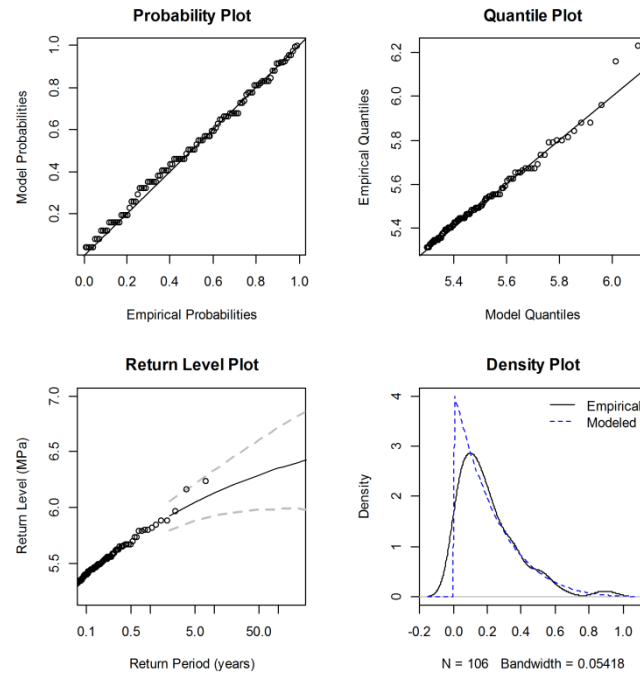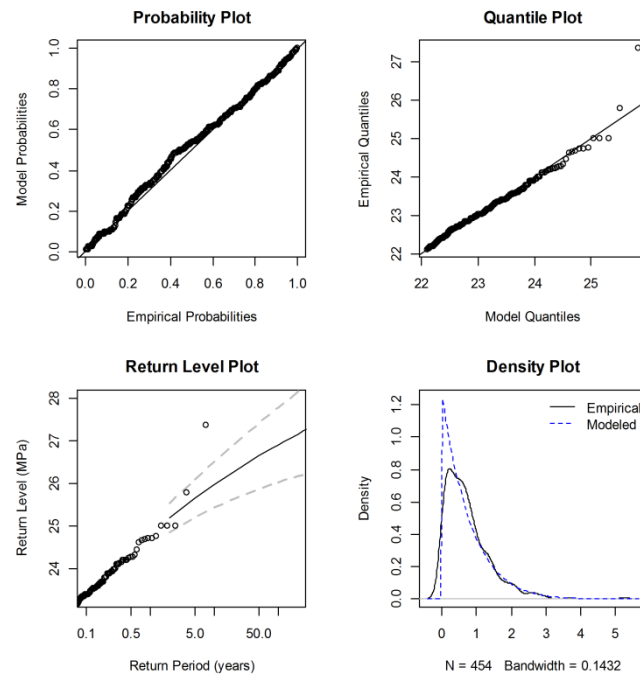
Fig. 7 Threshold selection for POT model of daily maximum railway-induced stresses

(a) Highway-induced stresses

(b) Railway-induced stresses

Fig. 8 Diagnostic plots for GP fitting to traffic-induced stresses

5.3 Comparisons and discussions

5.3.1 Extrapolation results of two methods

A summary of the highway- and railway-induced extreme stresses with a return period of 120 years extrapolated by the BM approach and the POT approach, respectively, is given in Table 3. Both the estimates and the 95% confidence intervals are provided. It is observed that the extreme stresses extrapolated by the two methods are very close to each other, though the POT method used more data. It implies that the extrapolated extreme values are robust to the extrapolation technique. This conclusion coincides with that drawn by O'Brien *et al.* (2015) who concluded that the accuracy of the extrapolated characteristic value is more dependent on data quality and less on extrapolation technique adopted.

Both the GEV and GP models fit well to the extremes of the measured stresses (Figs. 6 and 8). For the railway-induced stresses, an extreme of extremes is observed (Fig. 5(b)). By examination of the strain data measured at the railway beams, it is found that this extreme was caused by two trains concurrently meeting near the measured deck section. Being a true extreme data point, it has not been excluded from the extreme stress dataset.

As stated in section 2.1, the GEV and GP distributions resulting from the same dataset are intimately related and share the same shape parameter ξ. That is to say, the estimated parameter ξ in the GEV and GP models should be the same theoretically. Probably because of the richness and good quality of the monitoring data, the estimated values of ξ for the GEV and GP distributions of the extreme stresses in this study are exactly the same. The shape parameter in the two extreme value models for the highway-induced stresses is estimated identically as -0.15, and it is identically -0.09 in the two models for the railway-induced stresses.

The extrapolated highway- and railway-induced extreme stresses with a return period of 120 years are not significantly larger than the maximum data values collected in the measurement periods (nine years). The maximum highway- and railway-induced stresses measured are 6.23 and 27.36 MPa respectively, while the extrapolated extremes for these two types of stresses obtained by the BM approach are 6.43 MPa with a 95% confidence interval of [6.21, 7.07] and 27.21 MPa with a 95% confidence interval of [26.58, 29.23]. They are reasonable because both the railway traffic and the highway traffic on the TMB are governed by regulations as stated in section 3.1.

5.3.2 Comparison of extrapolated extremes with design values

The design live loadings of the TMB are determined by the United Kingdom Department of Transport Standard BD 37/88 with amendments to suit the traffic conditions predicted for the TMB. The highway loading adopted is HA and 45 units of HB loading applied to the roadway deck in the severest configuration. The design railway loading for the TMB is an 8-car train with a gross weight of 544 tonnes. These two kinds of design live loads are applied respectively to a 3D FEM of the TMB to obtain the stress responses.

The influence line of stress at the deck location with the strain gauge SSTLS09 is shown in Fig. 9. The positive value means tensile strain. It is obtained by a vehicle with a gross weight of 1 tonne running on the upper deck in the lane closest to SSTLS09. The influence lines owing to a vehicle passing over other lanes can be obtained in a similar way. It can be observed from Fig. 9 that the length of distributed load to generate large load effect (stress) in the concerned point is approximately 250 m (100 m on the left and 150 m on the right). The portion of influence line spanning this length is sharp, so the most adverse condition is when several heavy trucks are positioned at the desired region. The design highway loads are then applied to the six lanes on the

upper deck accordingly to compute the stress. The calculated design stress is obtained as 76.77 MPa. In summary, the predicted highway-induced extreme stress with a return period of 120 years is much less than the design value.

In daily operation, the vehicles are mostly distributed along the whole length of the bridge, rather than just along the adverse region. When the design highway loading is applied to the whole length of the bridge, the calculated stress at the same deck location is only 2.79 MPa. The reason for such a small value is that the stress generated by the uniform distribution load (UDL) of HA loading along the adverse length has been nearly offset by that generated by UDL along the favorable length. The stress is mainly caused by the HB loading or the knife edge load (KEL) multiplied by proper HA lane factors as suggested in the design code. This implies that when assessing in-service condition of the bridge, it may not be appropriate to use the 45 units of HB loading or the KEL of 120 kN as adopted in the design. The reason is that in in-service condition assessment, the daily operational situation (i.e. the highway loads are considered to be distributed along the full length of the bridge) is closer to reality. The HB loading or the KEL is preferably determined according to the loadings and distributions of site-specific heavy trucks. A live load model for in-service condition assessment of the TMB will be developed in next-step research by using the long-term SHM data.
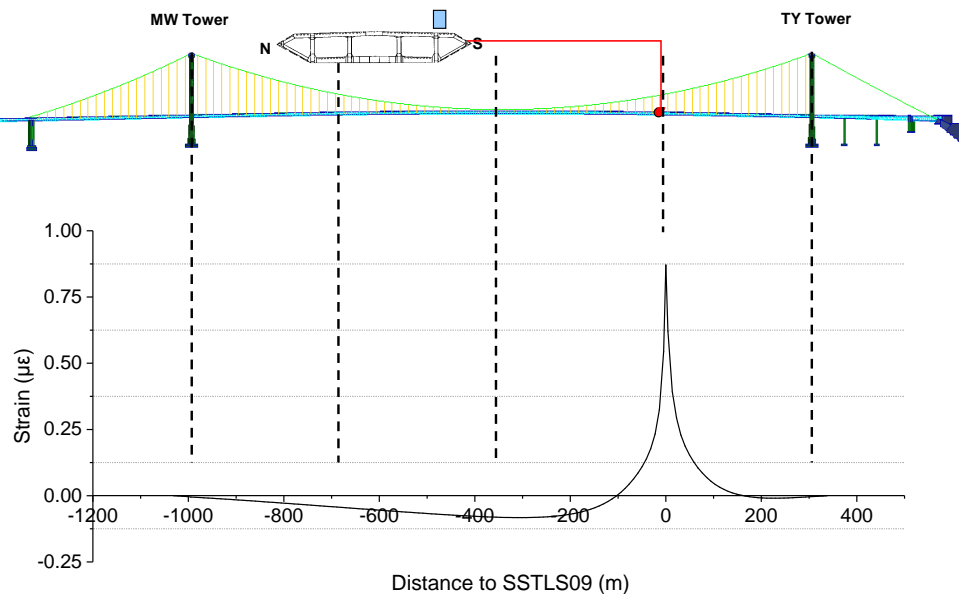

Fig. 9 Influence line of stress at deck location with strain gauge SSTLS09

Table 3 Estimate and 95% confidence interval of stresses with a return period of 120 years

	Estimate (MPa)		95% confidence interval (MPa)	
	Highway stress	Railway stress	Highway stress	Railway stress
GEV	6.43	27.21	(6.21, 7.07)	(26.58, 29.23)
GP	6.36	27.25	(6.21, 7.10)	(26.58, 29.40)

In the FEM, loads simulating two 8-car trains are applied on the rail tracks side by side. The axle distances and axle loads of the trains comply with the specifications of BD 37/88. The computed stress in the deck location with SSTLS09 is 38.98 MPa. As such, the extrapolated railway-induced extreme stress with a return period of 120 years is about 70% of the design value. The yield strength of the structural steel for the longitudinal truss is 355 MPa, and the strength for the serviceability limit state (SLS) evaluation is 154 MPa. It can be concluded from the above comparisons that the characteristic values of the traffic-induced extreme stresses with a return period equal to the bridge's design life are much lower than the design values and the material strength. Therefore, the live load design of the bridge is conservative and the bridge is currently in a good operational condition. Two or more strain gauges have been installed on each of the instrumented truss members of the TMB; thus the inner forces experienced in each truss member and experienced by the whole cross-section of the deck can be further evaluated from the measured strain data. The characteristic values of these inner forces can also be extrapolated following the same way as described in this paper.

6. Conclusions

This paper addressed the extrapolation of extreme TLEs on bridges based on long-term SHM data for reliable bridge condition assessment. The instrumented TMB which carries both highway and railway traffic was taken as a testbed for this study. Making use of the EVT, the extreme stresses induced by highway and railway traffic were extrapolated respectively from the long-term strain monitoring data. Both the BM and POT approaches were employed to extrapolate and compare the extreme stresses in a return period of 120 years. The extrapolated extreme stresses were also compared with the values generated by design live loadings. With a non-deterioration assumption, this paper comes to the following conclusions:

- The shape factors obtained from the GEV and GP fittings to the extreme stresses are the same, as theoretically expected. The extrapolated characteristic values of the extreme stresses are robust to the two extrapolation techniques adopted;
- The extrapolated extreme stresses with a return period of 120 years are not significantly larger than the maximum data values measured in the period studied. It is reasonable because both the railway traffic and the highway traffic on the TMB are well controlled by regulations;
- The extrapolated traffic-induced extreme stresses with a return period equal to the bridge's design life are much lower than the values generated by design live loads. It validates a safe and conservative design of traffic loads and a safe traffic-loading condition of the bridge at present;
- In in-service condition assessment of long-span bridges, it may not be appropriate to adopt the live load models used in the design. The site-specific live load models derived by using long-term SHM data are desired.

Acknowledgments

long-term structural health monitoring data of the Tsing Ma Bridge.

References

American Association of State Highway and Transportation Officials (AASHTO) (2011), *Manual for Bridge Evaluation*, Washington, USA.

American Association of State Highway and Transportation Officials (AASHTO) (2015), *LRFD Bridge Design Specifications*, Washington, USA.

Canadian Standards Association (CSA) (2006), *Canadian Highway Bridge Design Code*, Toronto, Canada.

Bailey, S.F. (1996), "Basic principles and load models for the structural safety evaluation of existing road bridges", *Ph.D. Dissertation*, University of Southampton, Southampton, UK.

Bailey, S.F. and Bez, R. (1999), "Site specific probability distribution of extreme traffic action effects", *Probabilist. Eng. Mech.*, **14**(1), 19–26.

Balkema, A.A. and De Haan, L. (1974), "Residual life time at great age", *Ann. Probab.*, **2**(5), 792-804.

Beirlant, J., Goegebeur, Y., Segers, J. and Teugels, J. (2006), *Statistics of Extremes: Theory and Applications*, John Wiley and Sons, Chichester, UK.

Caprani, C.C. (2005), "Probalistic analysis of highway bridge traffic loading", *Ph.D. Dissertation*, Dublin Institute of Technology, Dublin, Ireland.

Caprani, C.C., O'Brien, E.J. and McLachlan, G.J. (2008), "Characteristic traffic load effects from a mixture of loading events on short to medium span bridges", *Struct. Saf.*, **30**(5), 394-404.

Castillo, E. (1988), *Extreme Value Theory in Engineering*, Academic Press, San Diego, USA.

Chan, T.H.T., Miao, T.J. and Ashebo, D.B. (2005), "Statistical models from weigh-in-motion data", *Struct. Eng. Mech.*, **20**(1), 85-110.

Coles, S. (2001), *An Introduction to Statistical Modeling of Extreme Values*, Springer, London, UK.

Crespo-Minguillón, C. and Casas, J.R. (1997), "A comprehensive traffic load model for bridge safety checking", *Struct. Saf.*, **19**(4), 339-359.

Enright, B. (2010), "Simulation of traffic loading on highway bridges", *Ph.D. Dissertation*, Dublin Institute of Technology, Dublin, Ireland.

Getachew, A. (2003), "Traffic load effects on bridges, statistical analysis of collected and Monte Carlo simulated data", *Ph.D. Dissertation*, Royal Institute of Technology, Stockholm, Sweden.

Gilli, M. (2006), "An application of extreme value theory for measuring financial risk", *Comput. Econ.*, **27**(2-3), 207-228.

Gilleland, E. and Katz, R.W. (2011), "New software to analyze how extremes change over time", *Eos*, **92**(2), 13–14.

Gindy, M. and Nassif, H.H. (2006), "Comparison of traffic load models based on simulation and measured data", *Proceedings of the Joint International Conference on Computing and Decision Making in Civil Engineering*, Montreal, Canada.

Grave, S. (2002), "Modelling of site-specific traffic loading on short to medium span bridges", *Ph.D. Dissertation*, Trinity College Dublin, Dublin, Ireland.

Gumbel, E.J. (1958), *Extreme Value Theory*, Columbia University Press, New York, USA.

Harris, R. (1996), "Gumbel re-visited-a new look at extreme value statistics applied to wind speeds", *J. Wind Eng. Ind. Aerod.*, **59**(1), 1-22.

Holmes, J. and Moriarty, W. (1999), "Application of the generalized Pareto distribution to extreme value analysis in wind engineering", *J. Wind Eng. Ind. Aerod.*, **83**(1), 1-10.

James, G. (2003), "Analysis of traffic load effects an railway bridges", *Ph.D. Dissertation*, Royal Institute of Technology, Sweden.

Jenkinson, A.F. (1955), "The frequency distribution of the annual maximum (or minimum) values of meteorological elements", *Q. J. Roy. Meteor. Soc.*, **81**(348), 158-171.

Katz, R.W., Parlange, M.B. and Naveau, P. (2002), "Statistics of extremes in hydrology", *Adv. Water Resour.*,

25(8), 1287-1304.

Ko, J.M. and Ni, Y.Q. (2005), "Technology developments in structural health monitoring of large-scale bridges", *Eng. Struct.*, **27**(12), 1715-1725.

Leadbetter, M.R., Lindgren, G. and Rootzén, H. (2012), *Extremes and Related Properties of Random Sequences and Processes*, Springer-Verlag, New York, USA.

Lubliner, J. (2008), *Plasticity Theory*, Courier Corporation, New York, USA.

Messervey, T.B., Frangopol, D.M. and Casciati, S. (2011), "Application of the statistics of extremes to the reliability assessment and performance prediction of monitored highway bridges", *Struct. Infrastruct. E.*, **7**(1-2), 87-99.

Miao, T.J. and Chan, T.H.T. (2002), "Bridge live load models from WIM data", *Eng. Struct.*, **24**(8), 1071-1084.

Ni, Y.Q., Wong, K.Y. and Xia, Y. (2011), "Health checks through landmark bridges to sky-high structures", *Adv. Struct. Eng.*, **14**(1), 103-119.

Ni, Y.Q., Xia, H.W., Wong, K.Y. and Ko, J.M. (2012), "In-service condition assessment of bridge deck using long-term monitoring data of strain response", *J. Bridge Eng.*, **17**(6), 876-885.

Ni, Y.Q. and Xia, Y.X. (2016), "Strain-based condition assessment of a suspension bridge instrumented with structural health monitoring system", *Int. J. Struct. Stab. Dy.*, **16**(4), Paper No. 1640027 (23 pages).

O'Brien, E., Schmidt, F., Hajializadeh, D., Zhou, X.Y., Enright, B., Caprani, C., Wilson, S. and Sheils, E. (2015), "A review of probabilistic methods of assessment of load effects in bridges", *Struct. Saf.*, **53**, 44-56.

O'Connor, A.J. (2001), "Probabilistic traffic load modelling for highway bridges", *Ph.D. Dissertation*, Dublin Institute of Technology, Dublin, Ireland.

Pickands III, J. (1975), "Statistical inference using extreme order statistics", *Ann. Stat.*, **3**(1), 119-131.

Poon, S.H., Rockinger, M. and Tawn, J. (2004), "Extreme value dependence in financial markets: diagnostics, models, and financial implications", *Rev. Financ. Stud.*, **17**(2), 581-610.

R Development Core Team (2014), *R: A Language and Environment for Statistical Computing*, Vienna, Austria.

Reiss, R.D., Thomas, M. and Reiss, R. (2001), *Statistical Analysis of Extreme Values*, Springer Basel AG, Washington D.C., USA.

Simiu, E., Heckert, N., Filliben, J. and Johnson, S. (2001), "Extreme wind load estimates based on the Gumbel distribution of dynamic pressures: an assessment", *Struct. Saf.*, **23**(3), 221-229.

Tawn, J.A. (1990), "Modelling multivariate extreme value distributions", *Biometrika*, **77**(2), 245-253.

Treacy, M.A., Brühwiler, E. and Caprani, C.C. (2014), "Monitoring of traffic action local effects in highway bridge deck slabs and the influence of measurement duration on extreme value estimates", *Struct. Infrastruct. E.*, **10**(12), 1555-1572.

Tsimplis, M. and Blackman, D. (1997), "Extreme sea-level distribution and return periods in the Aegean and Ionian Seas", *Estuar. Coast. Shelf S.*, **44**(1), 79-89.

Wong, K.Y. (2004), "Instrumentation and health monitoring of cable-supported bridges", *Struct. Control Health.*, **11**(2), 91-124.

Xia, H.W., Ni, Y.Q., Wong, K.Y. and Ko, J.M. (2012), "Reliability-based condition assessment of in-service bridges using mixture distribution models", *Comput.Struct.*, **106**, 204-213.